

Carboxylate Anion Diminishes Chloride Transport through a Synthetic, Self-Assembled Transmembrane Pore

Lei You,^[a] Riccardo Ferdani,^[b] Ruiqiong Li,^[a] Joseph P. Kramer,^[b]
Rudolph Ernst K. Winter,^[b] and George W. Gokel^{*,[a, b, c]}

Abstract: Six amphiphilic heptapeptides with the structure $(C_{18}H_{37})_2NCO-CH_2OCH_2CO-(Gly)_3-Pro-(Gly)_n-(Glx)-(Gly)_m-O(CH_2)_6CH_3$, in which Glx represents glutamic acid or its benzyl ester and $n+m=2$, have been studied. In addition, the glutamate residue in the GGGPGGE sequence was esterified by fluorescent 1-pyrenemethanol. These compounds insert into phospholipid bilayers and form anion-conducting pores. Hill plots based on carboxyfluorescein release indicate that the pores are at least dimeric. Studies that involved ion-selective electrode tech-

niques showed that transport of chloride varied with the position of glutamate within the peptide chain and whether glutamic acid was present as the free acid or its benzyl ester. Chloride transport activity was significantly higher for the glutamate esters than for free carboxylates irrespective of the glutamate position. Activity was highest when the glutamate residue in

$\sim(Gly)_3-Pro-(Xxx)_3\sim$ was closest to the C terminus of the peptide. A fluorescent pyrene residue was introduced to probe the aggregation state of the amphiphile. The selectivity of the pore for Cl^- over K^+ was maintained even when the carboxylate anion was present within it. Complexation of Cl^- by the ionophoric peptides was confirmed by negative ion mass spectrometry. Planar bilayer voltage clamp experiments confirmed that pores with more than one conductance state may form in these dynamic, self-assembled pores.

Keywords: anion transport • membranes • peptides • self-assembly • supramolecular chemistry

Introduction

Over the last ten years, numerous anion-complexing agents^[1,2] have been designed, prepared, and studied.^[3,4,5] In many cases, the ability of these receptor molecules to complex anions has been characterized by X-ray crystallography. Solution complexation of various anions has also been studied for cyclic^[6] and acyclic receptors.^[7] Our particular interest has been in designing molecules that can form pores in phospholipid bilayers and not only complex anions, but transport them across a membrane.^[8] The successful forma-

tion of a transmembrane, anion-conducting pore would mimic some functions of the CIC family of chloride-transporting proteins.^[9,10,11,12]

The first solid-state structure of a CIC protein was reported in 2002.^[13] The amino acid sequence G(K/R)EGP at positions 146 to 150, which is conserved in CIC Cl^- transporting proteins, was thought to be part of the conductance pore. Subsequent study led to the proposal that chloride transport was gated, at least in part, by a glutamate residue at position 148 (E-148).^[14] The solid-state structure of a Glu¹⁴⁸→Ala¹⁴⁸ mutant revealed a fully open channel. The ion path suggested by structural studies for chloride transport is complex and involves interactions with at least a main-chain amide NH, tyrosine and serine side chains, and a phenylalanine.^[14]

Glutamic acid has a side chain carboxyl pK_a of ≈ 4.3 . We presume that there is a significant concentration of water within the self-assembled pores. At physiological pH, the glutamate carboxyl group should be completely deprotonated. A carboxylate anion should certainly repel a chloride anion, but the effect of a carboxylate anion present within a pore on transport is less clear. Within a pore, a carboxyl group could repel Cl^- and prevent passage of this ion. Alternatively, the combination of negative charges could cause

[a] L. You, R. Li, Prof. Dr. G. W. Gokel
Department of Chemistry, Washington University
1 Brookings Drive, St. Louis, MO 63130 (USA)
Fax: (+1) 314-516-5321
E-mail: gokelg@umsl.edu

[b] Dr. R. Ferdani, Dr. J. P. Kramer, Dr. R. E. K. Winter,
Prof. Dr. G. W. Gokel
Departments of Chemistry & Biochemistry and Biology
University of Missouri—St. Louis, St. Louis, MO 63121 (USA)

[c] Prof. Dr. G. W. Gokel
Center for Nanoscience, University of Missouri—St. Louis
St. Louis, MO 63121 (USA)

the pore to collapse. A third possibility is that if the Cl^- concentration gradient was large, the carboxyl could be repelled by Cl^- , the pore opened to a wide diameter, and ions (possibly of both charge types) could traverse the membrane. This would be a simple charge-based gating mechanism. A challenge is to develop a dynamic transport system that functions within the bilayer and incorporates features of complex modern proteins.

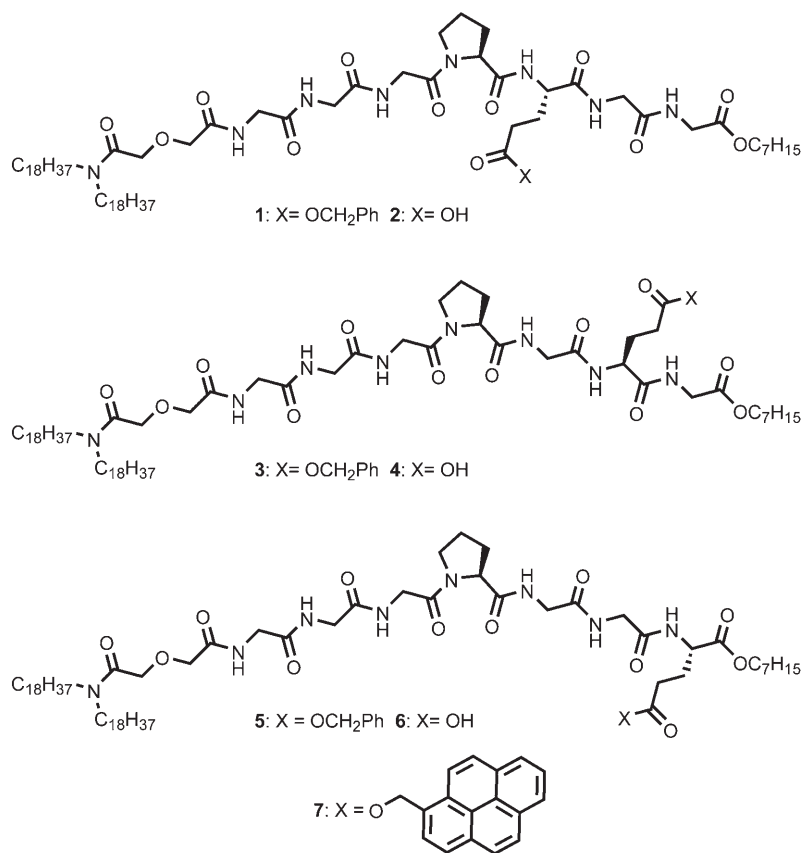
In extensive previous studies,^[15] we have found that compounds of the general form $(\text{C}_n\text{H}_{2n+1})_2\text{NCOCH}_2\text{OCH}_2\text{CO}(\text{Gly})_3\text{-Pro}(\text{Gly})_3\text{-OR}$ insert in phospholipid liposomes to form a chloride-selective, ion-permeable pore. Variations in both the N- ($\text{C}_n\text{H}_{2n+1}$) and C-terminal (OR or NHR) alkyl groups altered the properties of the pores that formed.^[15c,e,g] Studies of carboxyfluorescein anion (CF^-) release from liposomes mediated by these compounds suggested that pore formation requires at least a dimer aggregate.^[15j] These synthetic peptides have also been shown to bind Cl^- ions in CDCl_3 in a cation-dependent fashion.^[15g,k]

In the work presented herein, we have varied the triad of amino acids on the C-terminal side of proline in heptapeptides GGGPXXX. Glycines in positions five to seven were systematically replaced by either glutamic acid or by its benzyl ester. This modification permitted us to assess the effect of a negative charge in each of the three "X" positions and to compare it with the presence of a sterically similar, but uncharged, side chain. Glutamic acid, rather than aspartic acid, was chosen for this study because it is glutamate that is present in the putative ion pathway of the CIC proteins.

Results and Discussion

Compounds used in the study: Seven amphiphilic heptapeptides of the type known to form chloride-conducting pores^[11] were prepared for use in the present study. Six of these compounds (**1–6**) all have the basic structure $\sim(\text{Gly})_3\text{-Pro}(\text{Xxx})_3\sim$. A seventh (**7**), discussed below, is a fluorescent analogue of **5**. The sequence was inspired by two observations. First, the GKxGP sequence, noted above as G(K/R)EGP, was conserved in the CIC transporter ion path. Fur-

ther, hinge bend sequences involving proline were typically GxxP. The simplest emulation of GxxP is GGGP, which was employed as $\sim(\text{Gly})_3\text{-Pro}(\text{Gly})_3\sim$, as the first example in this system.



8: $(\text{C}_{18}\text{H}_{37})_2\text{NCOCH}_2\text{OCH}_2\text{CO}(\text{Gly})_3\text{-Pro}(\text{Gly})_3\text{-O}(\text{CH}_2)_7\text{CH}_3$

At the C-terminal side of proline, triglycine ($\sim\text{GlyGlyGly}\sim$) was systematically replaced by $\sim\text{GlxGlyGly}\sim$, $\sim\text{GlyGlxGly}\sim$, or $\sim\text{GlyGlyGlx}\sim$, in which Glx represents both glutamic acid and its benzyl ester. The suite of compounds thus comprises three pairs of related structures: **1** and **2**, **3** and **4**, and **5** and **6**. The first pair (**1** and **2**) can be described by the general formula $(\text{C}_{18}\text{H}_{37})_2\text{NCOCH}_2\text{OCH}_2\text{CO}(\text{Gly})_3\text{-Pro-Glx}(\text{Gly})_2\text{-O}(\text{CH}_2)_6\text{CH}_3$. In **1**, Glx is glutamic acid and its side chain carboxyl group is benzylated. In **2**, Glx is glutamic acid (Glu), which has a free carboxyl group. Similarly, peptide sequences for **3** and **4** are $(\text{Gly})_3\text{-Pro-Gly-Glx-Gly}$ in which Glx is benzylated Glu in **3** and Glu in **4**. The final two peptides, **5** and **6**, have the sequence $(\text{Gly})_3\text{-Pro-Gly-Gly-Glx}$ in which Glx is benzylated Glu in **5**, Glu in **6**, and in **7** Glx is Glu that has been esterified by 1-pyrenemethanol. All eight heptapeptides (**1–8**), have the $(\text{C}_{18}\text{H}_{37})_2\text{NCOCH}_2\text{OCH}_2\text{CO}\sim$ group at the N terminus of the peptide.

The twin octadecyl chains in **1–8** are intended to commingle with the fatty acid chains in the bilayer, thus anchoring

the amphiphilic peptide within the membrane^[16] and the C-terminal heptyl group serves as a secondary anchor.^[15c] From an evolutionary perspective, we surmise that the earliest transmembrane pores were formed by molecules that resembled the membrane monomers themselves. In modern bilayers, the monomers are phospholipids. We thus incorporated the diglycolyl residue as a spacer and connector that links the twin hydrocarbon chains to the peptide. Diglycolic acid ($O(CH_2COOH)_2$) was chosen because it can be easily converted into its anhydride, which can then be opened by treatment with a secondary amine (R_2NH) to give $R_2NCOCH_2OCH_2COOH$. Equally important, however, is the fact that the polar atoms in the diglycolyl residue are positioned to emulate the polar elements of the glycerol subunit of a phospholipid.

The alkyl chain span (C-18→N) is $\approx 22.4 \text{ \AA}$ and the diglycolic acid chain adds $\approx 6.4 \text{ \AA}$ (total length $\approx 29 \text{ \AA}$). Together with the diglycolic acid subunit, the twin chains approximate the length and polarity of the diacylglycerol unit of phospholipids. The span of the insulator or hydrocarbon regime of a bilayer is typically estimated to be 30 to 35 \AA . The hydrocarbon chains of **1** to **8** will not span this distance, but a pore can form by rearrangement of the phospholipid monomer head groups in the lower leaflet of the bilayer.^[17] Both Cl^- and CF^- release are mediated by



Hill plots based on the concentration dependence of ion release showed that a minimum of two amphiphilic peptides were required for ions to pass through a liposomal bilayer.^[15h] Thus, pore formation can occur by insertion of the amphiphiles into the outer leaflet of the bilayer. This will place glutamate residues in the chloride ion pathway; this is illustrated schematically in Figure 1.

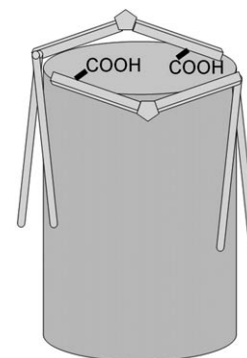
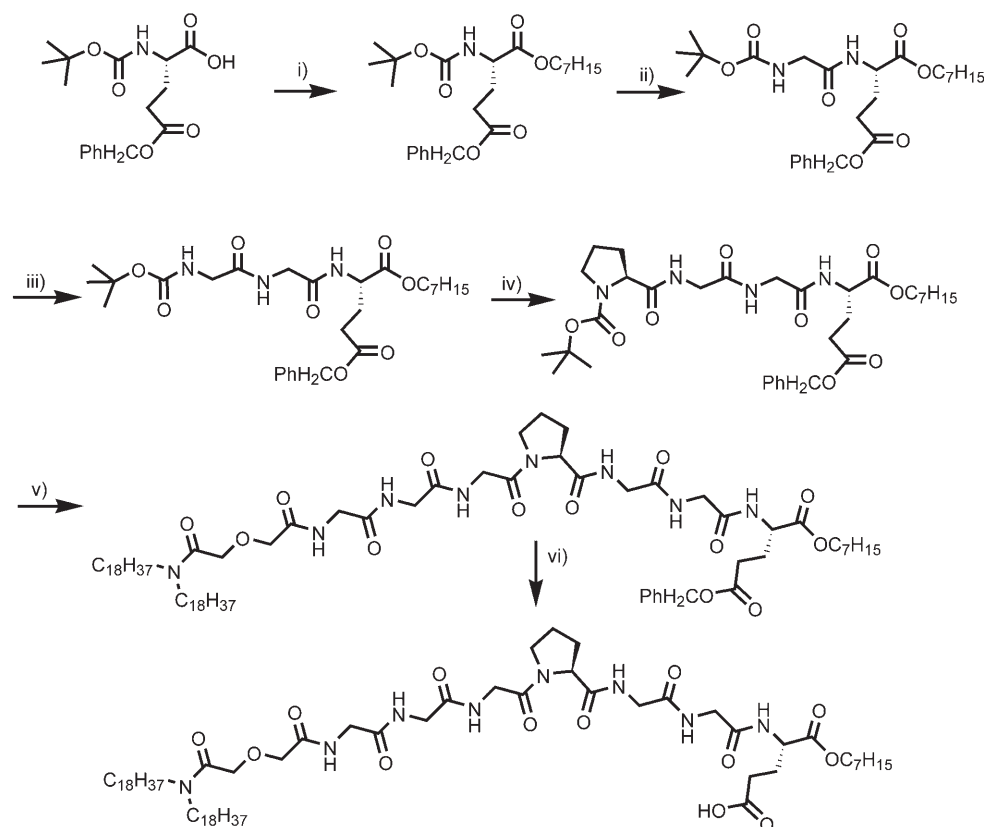


Figure 1. Schematic representation of a pore formed by the association of two amphiphilic heptapeptides.

Synthetic access to compounds

1–7: The series under study comprises three pairs of compounds, **1** and **2**, **3** and **4**, and **5** and **6**. Compound **7** is a pyrenyl ester analogue of **5**. The production of each of the free acids and esters within the series confronts similar synthetic issues. Thus, we show the preparation of **5** and **6**, the pair of compounds that have the $\sim(Gly)_3\text{-Pro-(Gly)}_2\text{Glx}\sim$ heptapeptide sequence, in Scheme 1.



Scheme 1. Synthesis of compounds **5** and **6**. i) 1-(3-dimethylaminopropyl)-3-ethyl carbodiimide hydrochloride (EDCI), 4-dimethylaminopyridine (DMAP), 1-heptanol, CH_2Cl_2 , 88%; ii) 1. HCl, dioxane, 2. Boc-Gly-OH, EDCI, 1-hydroxybenzotriazole (HOBt), Et_3N , CH_2Cl_2 , 76%; iii) 1. HCl, dioxane, 2. Boc-Gly-OH, EDCI, HOBt, Et_3N , CH_2Cl_2 , 84%; iv) 1. HCl, dioxane, 2. Boc-Pro-OH, EDCI, HOBt, Et_3N , CH_2Cl_2 , 74%; v) 1. HCl, dioxane, 2. $18_2DGA-GGG-OH$, EDCI, HOBt, Et_3N , CH_2Cl_2 , 47%; vi) 10% Pd/C, EtOH, H_2 , 93%.

2-*t*-Butoxycarbonylamino-pentanedioic acid 5-benzyl ester (*N*-Boc L-glutamic acid γ -benzyl ester) was esterified with *n*-heptanol, the *t*-Boc group was removed (HCl/dioxane), and the heptyl ester was coupled to *t*-Boc-Gly-OH. The resulting dipeptide was coupled to *t*-Boc-Gly-OH to give Boc-Gly-Gly-Glu(OCH₂Ph)-OC₇H₁₅ after Boc deprotection. Sequential reaction with HCl/dioxane and then *t*-Boc-Pro-OH gave the *t*-Boc-protected tetrapeptide Pro-(Gly)₂-Glu. We have previously reported the preparation of (C₁₈H₃₇)₂NCOCH₂OCH₂CO-(Gly)₃-OH, which was coupled to the deprotected tetrapeptide to form diester **5**.^[11d] The side chain benzyl ester in **5** was hydrogenolytically removed to give **6**. Details of the preparation of compounds **1** to **7** are given in the Experimental Section.

Chloride release from liposomes mediated by 1–6: Chloride transport can be assessed in various ways. Planar bilayer clamp studies give the most detailed picture of a conductance pore, but the method is complex and time consuming. For the compounds described herein, we used an assay in which Cl⁻ release from liposomes was detected by an Accumet chloride-selective electrode. Thus, liposomes (200 nm average diameter) were prepared from a 7:3 (w/w) mixture of 1,2-dioleoyl-*sn*-glycero-3-phosphocholine (DOPC) and 1,2-dioleoyl-*sn*-glycero-3-phosphate (DOPA) as described in the Experimental Section. The vesicles were loaded with KCl (600 mM) in HEPES buffer (pH 7). The external buffer was chloride free K₂SO₄ (400 mM) in HEPES (pH 7). With the electrode inserted into the aqueous liposome suspension, the ionophore under study was introduced as a solution in 2-propanol and the response of the electrode was recorded over 1800 s.

Typically, the chloride electrode began to respond to ion release within five seconds after ionophore addition. Data collection is automated and a value was typically recorded every second. At the conclusion of an experiment, Triton X-100 detergent was added to lyse the vesicles and a final value was determined for chloride concentration. This value was arbitrarily set to one and the release data presented are the fraction of total chloride measured after vesicular lysis. Each data set is the average of at least three independent experiments. Typical results are shown in Figure 2 for **3**, **4**, **5** and **6**.

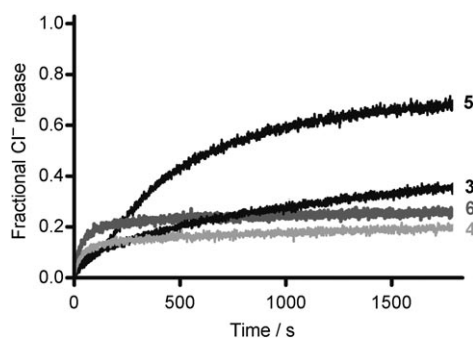


Figure 2. Chloride release from phospholipid liposomes mediated by **3** and **4**, **5** and **6** (lipids (0.31 mM), compounds (65 μ M), pH 7.0).

The chloride release data in Figure 2 show that initial chloride transport is similar (0–250 s) for **3** and **4**. We infer that the insertion of either compound into the bilayer occurs with similar dynamics. In contrast with the initial behavior, Cl⁻ release after 1800 s is significantly higher for **3** than for **4**. Structurally, these compounds differ only by the presence or absence of the benzyl ester on the glutamic acid residue at position 6 in the peptide. Although the modes of insertion and pore formation remain speculative, it is clear that **4** must present a negative charge in or near the pore and **3** does not. If the pore is dimeric or oligomeric, more than one negative charge will be present proximate to the pore (see Figure 1). The side chain carboxyl of glutamic acid is reported to have a pK_a value of 4.32, so it will be completely ionized beyond about pH 6.8; the experiment is conducted at pH 7.

Compounds **6** and **5** are identical (sequence: GGGPGGE) except that the former is the free acid and the latter is its benzyl ester. Thus, the glutamate residue is at the C-terminal (position 7) end of the heptapeptide. Compound **4** is a free acid with the peptide sequence GGGPGEG; chloride release for free acids **4** and **6** is very similar, both in terms of curve shape and ultimate ion release. Chloride release mediated by benzyl ester **5**, however, is about twice (0.65 vs. 0.32) that observed for the benzyl ester of **4**, that is, **3**. The curve shapes exhibited by ion release can be difficult to interpret, but either insertion or the initial organization into a pore clearly occurs differently for esters **5** and **3**.

The chloride transport activity of glutamic acid derivative **2** (G₃PEGG) is slightly less than, but similar to, that shown above for **4** (G₃PGEG) and **6** (G₃PGGE). In all three cases, however, the ability of free acid compounds **2**, **4**, and **6** to transport Cl⁻ is less than that observed for esterified analogues **1**, **3**, and **5**. We infer from this that the presence of one or more negative charges in the ion pathway impeded Cl⁻ entry into the pore and/or transport through it. In terms of electrostatic interactions, it seems reasonable that this should be so, although the curve shape does not reveal which, if either, of these variables is dominant. In the ClC channel, the Glu¹⁴⁸→Ala¹⁴⁸ mutation appeared to foster an open ion conduction pathway.^[18] The lower activity of **2**, **4**, and **6** (charged) than **1**, **3**, and **5** (neutral) suggests that the self-assembled pores described herein are similarly affected by a charge in the ion path.

Comparison of transport rates: Compounds **1–6** are similar in overall structure, but the variations in transport rates are significant. In addition, the curve shapes differ. In all cases, any divergence in the curve shapes occurs primarily in the first 0 to 300 seconds of observation. The various curve shapes must reflect differences in the rates of amphiphile insertions and the dynamics of pore formation. The details of these processes remain to be characterized, but the curves exhibit reasonably regular shapes, at least after this initial period.

Chloride ion release data are summarized in Table 1. Compound **5** showed the greatest ion release at the arbitrarily selected time point of 1500 s. Its release value at 1500 s

Table 1. Comparison of fractional chloride release from liposomes mediated by **1–6** at 1500 s

Compound	Peptide sequence	Release at 1500 s ^[a]	Relative rate ^[b]	% ^[c]
1	GGGPE(OCH ₂ Ph)GG	0.42	65	} 33 %
2	GGGPEGG	0.14	22	
3	GGGPGE(OCH ₂ Ph)G	0.32	49	} 62 %
4	GGGPGE	0.20	30	
5	GGGPGGE(OCH ₂ Ph)	0.65	100	} 38 %
6	GGGPGGE	0.25	38	

[a] Fraction of Cl⁻ detected after liposomal lysis. [b] Comparison of **1–6**; release for **5** arbitrarily set to 100. [c] Percentage of activity for the less effective compound in each pair.

was therefore set to 100 and the values shown in column 4 of Table 1 were calculated accordingly. Thus, 22 to 100 represents the overall range of chloride release values.

Thus far, the synthetic anion transporter (SAT) derivatives have not yielded crystals suitable for solid-state structural analysis. A detailed solution NMR analysis on (C₁₈H₃₇)₂N-COCH₂OCH₂CO-(Gly)₃-Pro-(Gly)₃-OCH₂Ph in the presence of Bu₄NCl showed a folded structure in which the amide NH hydrogen atoms on ⁵Gly and ⁷Gly strongly interact with chloride anions in homogeneous solution.^[15k,l] Both 1D and 2D NMR indicated that the amide protons of the fifth and seventh residues (i.e., the fourth and sixth glycines) are hydrogen bonded to Cl⁻ in solution in CDCl₃, but the NH of glycine-5 (the sixth residue) is not. Replacement of either glycine residue by glutamate will obviously have conformational consequences on this NH donor interaction. The data presented in Table 1 confirm that a Gly→Glu mutation at positions 5 (⁵Gly) or 7 (⁷Gly), alters the Cl⁻ transport rate more than a corresponding alteration at position 6.

To confirm the validity of comparisons between the amphiphile pairs **1–2**, **3–4**, and **5–6**, we computed the difference in transport rate for each pair at time values between 300 and 1500 s. This gave three 1200-point lines that are shown in Figure 3. Each of the three data sets is overlaid by a calculated second order fit. The scatter in each line is clearly modest and the calculated correlation factor (R²) is at least 0.91 in each case. We infer that although the dynamics of pore formation may vary, which is reflected in the 0 to 300 s time frame, ion release is reasonably consistent thereafter.

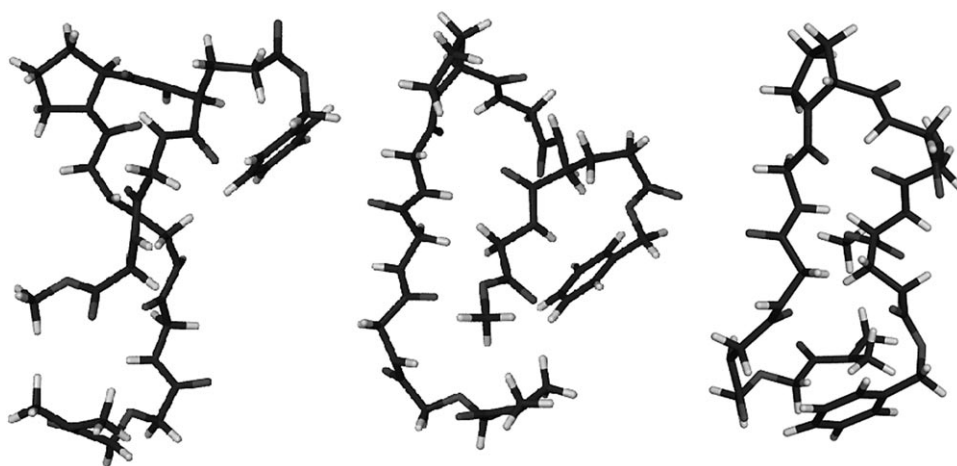


Figure 4. Calculated structures for **1** (left), **3** (center), and **5** (right).

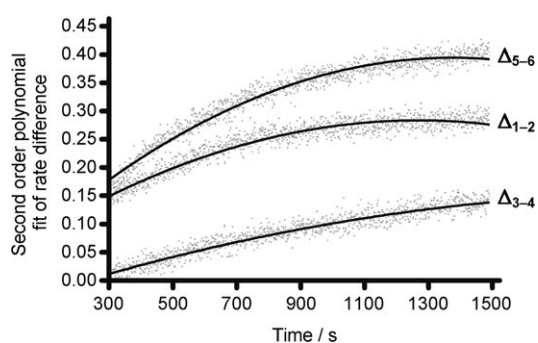


Figure 3. Difference in Cl⁻ release from liposomes for the amphiphile pairs **1–2** (middle, R²=0.92), **3–4** (bottom, R²=0.91), and **5–6** (top, R²=0.96). The solid line in each case is the calculated fit.

Comparison of ester compounds: In the ester series (**1**, **3**, and **5**), **5** is the most active and **3** is the least active Cl⁻ transporter. The presence of a bulky benzyl ester side chain is expected to alter the conformation of the peptide and to have an especially large effect when it is near either of the amide protons (⁵Gly or ⁷Gly), which were identified above as the key donor residues. We surmise that the benzyl group will have the greatest effect where it is most flexible (C terminus) and the least effect near the rigid proline. Computational studies were conducted by using Gaussian 03^[19] (gas phase, see the Experimental Section) to gain insight into this structural question.

The calculations were performed on analogues of (C₁₈H₃₇)₂N-COCH₂OCH₂CO-(Gly)₃-Pro-(Gly)₃-OCH₂Ph in which the N-terminal octadecyl alkyl chains and the C-terminal benzyl ester were replaced by methyl groups. This simplified the calculation, which was intended to focus on the heptapeptide chain. The structures that correspond to **1**, **3**, and **5** are arranged in Figure 4 with the proline residue at or near the apex of each structure. The N-terminal side of the chain descends from it to the left and the C-terminal chain, which includes the glutamate benzyl ester, appears at the right.

A key finding of the calculated structures (Figure 4) is that the benzyl group of **5** (right structure) may serve as an additional anchor to the bilayer. Assuming that a better anchored monomer contributes to a more stable conduction pore, then **5** should be superior to either **1** or **3** as an ion transporter. This accounts, at least in part, for the higher transport activity observed for **5** in this group of three closely related structures. It is interesting to note that the benzene ring in the peptide of **3** is very close to the amide NH of the sixth glycine (position-7, C terminus). The NMR results described above^[15k] clearly show that this NH is critical for binding Cl⁻. An NH... π hydrogen-bond contact between the benzyl ester and ⁷G_{NH} could further diminish the transport activity of **3** relative to **1** and **5** by hindering access of the transient chloride ion to the molecule.

Secondary anchor effect: The pores formed by molecules **1** to **6** are self-assembled. As such, the effect of residues that can help to anchor and/or organize the monomers in the bilayer is potentially very significant. Diglycolic acid is used in our SAT design as the glycerol-mimetic transition from the peptide to the N-terminal alkyl chain anchors. The similarity of diglycolic and glutamic acids to each other and to the glyceryl residue is apparent (Figure 5). It is plausible that glutamic acid could serve as a transitional component for a benzyl group anchor.

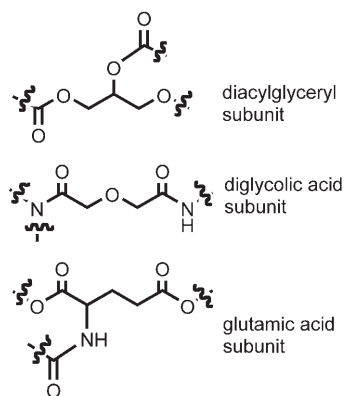


Figure 5. The structures of the diacylglycerol and diglycolic acid subunits, which are similar to that of the glutamic acid subunit.

It is interesting to note that Tirrell and co-workers have used a similar structural motif as an N-terminal midpolar regime mimetic.^[20] They have also observed antibiotic activity for their compounds.^[21] The peptides reported herein have not yet been screened for antibacterial activity, but our hydrophilic cation-selective channels have shown significant cytotoxicity.^[15]

Acid position on the heptapeptide chain: The chloride transport activity of free acids **2**, **4**, and **6** are all lower than their esterified analogues. Their transport efficacy increases almost linearly as the glutamate residue is moved from its

position adjacent to proline (**2**) towards the C terminus of the peptide. Thus, at 1800 s, the fractional Cl⁻ release values are 0.13 for **2**, 0.20 for **4**, and 0.25 for **6**. The release profiles (line shapes) are similar in all three cases (see Figures 2 and 3). Based simply on charge-charge repulsion, it seems reasonable that Cl⁻ transport would be hindered by encountering a negative charge within the pore. It was also plausible that charge-charge repulsions between Cl⁻ and carboxylate could force the self-assembled monomers apart, which results in making the pore larger, increasing ion flux, and reducing selectivity.

Anion versus cation transport: Early studies of (C₁₈H₃₇)₂N-COCH₂OCH₂CO-(Gly)₃-Pro-(Gly)₃-OCH₂Ph showed a minimum ten-fold selectivity for Cl⁻ over K⁺.^[15b] This information was obtained by the cumbersome planar bilayer conductance method. An alternative approach is to measure potassium efflux and compare it with chloride release data. Potassium cation transport experiments were conducted as described for the corresponding Cl⁻ experiments, except that the external buffer was a mixture of choline chloride (600 mM) and HEPES (10 mM) held at pH 7.0. Compounds **1** to **6** all mediated K⁺ release from DOPC/DOPA liposomes to a small extent. The most active chloride transporter (**5**) showed 12% K⁺ release at 1500 s compared with 65% for Cl⁻ release. The least active Cl⁻ transporter (**2**) showed approximately 1% K⁺ release compared with 14% Cl⁻ release at 1500 s. These data correspond to selectivity ratios of \approx 5:1 to 14:1 for Cl⁻ over K⁺. The key finding of this part of the study is that the self-assembled transmembrane pores remain Cl⁻ selective even when the free carboxylate anion is present within or proximate to the pore. A negatively charged side chain within the pore could electrostatically attract K⁺. Effective transport depends on both transient complexation and release. If K⁺ enters the pore, but is neither released nor blocks the pore, Cl⁻ transport will dominate and selectivity will be maintained. This explanation is consistent with our recent finding (unpublished) that a positive charge within the pore does not enhance anion transport.

Negative ion mass spectral study: Electrospray mass spectrometry (ES-MS) is a powerful structural tool that has been used relatively little to probe anion complexation.^[22,23] We have used it to characterize the SAT molecules and the Cl⁻ complexes that are the subject of this paper.

When (C₁₈H₃₇)₂N-COCH₂OCH₂CO-(Gly)₃-Pro-(Gly)₂-Glu-O(CH₂)₆CH₃ (**6**) in CH₃CN/2-PrOH (1:1 v/v) was sprayed, only two peaks with ion abundances greater than 20% were observed in the mass range 600 to 2400. The base peak was observed at *m/z* 1245.6 and corresponds to [6-H]⁻. The other peak in the spectrum occurred at *m/z* 1217.6 and corresponds to loss of a proton and CO from **6**. Loss of 28 mass units could correspond to CO or to ethylene. We were unable to find any precedent for this decomposition mode of glutamate in negative ion MS. There is, however, a report of CO loss from glutamic acid esters that

suggests it is CO rather than $\text{CH}_2=\text{CH}_2$ that is lost in the present case.^[24]

When a 1:3 molar ratio mixture of **6** and Cl^- was sprayed in CH_3CN , four major peaks were observed in the 1192 to 1314 mass range, m/z 1217.6 (46%), 1245.6 (100%), 1253.5 (18%), and 1281.5 (27%). These ions correspond to $[\mathbf{6}-\text{H}-28]^-$, $[\mathbf{6}-\text{H}]^-$, $[\mathbf{6}+\text{Cl}-28]^-$, and $[\mathbf{6}+\text{Cl}]^-$, respectively. As in the absence of Cl^- , the base peak is deprotonated **6**. Its complex with Cl^- has an abundance of 27%. This is a ratio of $[\mathbf{6}-\text{H}]^-/[\mathbf{6}+\text{Cl}]^-$ of $\approx 3.7:1$. This ratio was unchanged when the $\mathbf{6}/\text{Cl}^-$ molar ratio was increased from 1:3 to 1:12. Similarly, the decarboxylated derivative of **6** has a ratio of parent to complex of ≈ 2.4 .

Similar experiments were conducted for **5**. When a 1:3 molar ratio mixture of **5** and Bu_4NCl was sprayed, only two major peaks were detected above 1000, m/z 1343.6 (50%) and m/z 1371.6 (100%). These ions are $[\mathbf{5}+\text{Cl}-28]^-$ and $[\mathbf{5}+\text{Cl}]^-$, respectively. Of course, free neutral **5** cannot be detected by negative ion ES-MS.

It would be interesting to use ES-MS to observe the extent of complexation by **6** compared to its ester analogue **5**. Therefore, competition experiments were performed. A mixture of **5**, **6**, and Bu_4NCl (molar ratio 1:1:1) was sprayed. Six species were observed above 1000, 1217.6 (35%) $[\mathbf{6}-\text{H}-28]^-$, 1245.6 (100%) $[\mathbf{6}-\text{H}]^-$, 1253.5 (12%) $[\mathbf{6}+\text{Cl}-28]^-$, 1281.5 (20%) $[\mathbf{6}+\text{Cl}]^-$, 1343.6 (30%) $[\mathbf{5}+\text{Cl}-28]^-$, and 1371.6 (72%) $[\mathbf{5}+\text{Cl}]^-$. The results are shown in Figure 6. When a 1:1:12 molar ratio of **5**, **6**, and

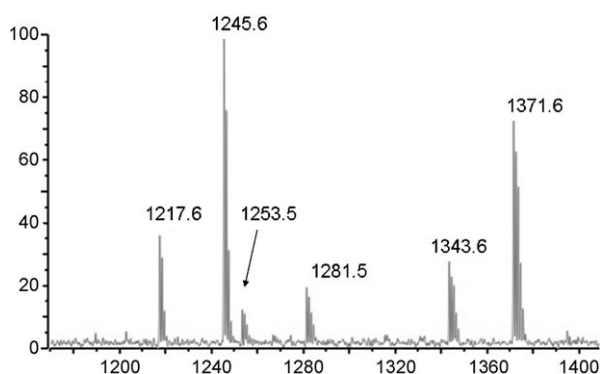


Figure 6. Negative ion mass spectrum of a 1:1 $\text{CH}_3\text{CN}/2\text{-PrOH}$ solution of $\mathbf{5}/\mathbf{6}/\text{Cl}^-$ in a 1:1:1 molar ratio.

Cl^- was used, the abundances for $[\mathbf{5}+\text{Cl}-28]^-$ and $[\mathbf{5}+\text{Cl}]^-$ increased to 47 and 94%, respectively. The peak intensity ratio for $[\mathbf{5}+\text{Cl}]^-$ over $[\mathbf{6}+\text{Cl}]^-$ was 3.6 for the 1:1:1 case and 4.7 when the molar ratios were 1:1:12.

It is apparent from these experiments that neutral **5** binds chloride anions. This result is expected from solution NMR results reported previously.^[15k] The results for **5** are in contrast with the behavior of **6**, which shows poor complexation behavior. Compound **6** is deprotonated to the extent that the negative charge will repel the chloride anion and result in poor binding. The poorer chloride binding, and

therefore, poorer ion-recognition capability of **6** compared with **5** may contribute to the lower transport efficacy of **6**.

Stoichiometry of pore formation: Chloride ion transport, as shown above, may be measured by using ion-selective electrodes. This method is reproducible and reliable, but sensitivity and the speed of the response are both limited. Carboxyfluorescein (CF^-) is an anion whose efflux from vesicles can be quantitatively monitored by fluorescence techniques.^[15a] The increased sensitivity also permits a broader concentration range to be surveyed than that for chloride release. Chloride and carboxyfluorescein may seem to be too different for comparison, but they have behaved similarly in a number of previous studies.^[15h]

Release of CF^- from DOPC/DOPA liposomes (see the Experimental Section) was monitored over a concentration range from 0.99 to $7.86 \mu\text{M}$. The ion-release data are shown in Figure 7a. Carboxyfluorescein release is consistent and

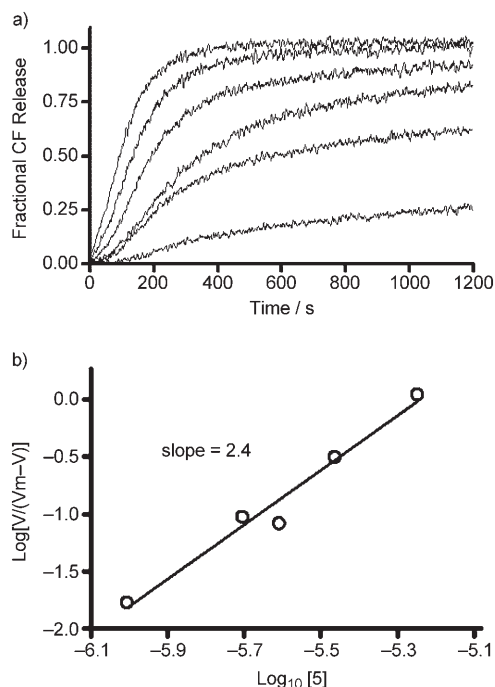


Figure 7. a) Carboxyfluorescein release from DOPC:DOPA vesicles mediated by **5** at the following concentrations (bottom to top): 0.99, 1.98, 2.47, 3.45, 5.66, and $7.86 \mu\text{M}$. b) Hill plot of CF release by **5**.

concentration dependent. The Hill equation^[25] was applied to the release data to determine the minimum number of monomers required for pore formation. The plot is shown in the Figure 7b; the slope of 2.4 suggests that at least two monomers are required, although more amphiphiles may be present in some pores.

Previous compounds of the general type $\text{R}^1\text{NCOCH}_2\text{OCH}_2\text{CO}-(\text{Gly})_3\text{-Pro}-(\text{Gly})_3\text{-OR}^2$, which have been studied, to date, formed pores that were at least dimeric.^[15a] Additional evidence for dimeric pore formation was acquired by covalently linking two amphiphilic monomers

either at the two C- or N-terminal ends.^[15j] The latter study is strongly suggestive that dimeric pore formation occurs, but is limited by the C-terminal to C-terminal and N-terminal to N-terminal linkages. In fact, the organization of the dimer pore may occur in a C-terminal to N-terminal fashion, as intuition suggests. To date, there is no direct experimental evidence to confirm a C→N organization in the bilayer. It should be noted, however, that both the C–C and N–N *pseudo*-dimers mediated Cl[−] release from liposomes more effectively than twice the concentration of monomers.^[15j]

We note that the Cl[−] and CF[−] release experiments were run under different conditions because the anions differ in structure and presumably in hydration state. These differences notwithstanding, the line shapes observed for release of these two ions are similar. Further, separate studies in which the two anions were compared, revealed comparable release profiles from vesicles when mediated by this family of ionophores.^[15h]

Fluorescent heptapeptide monomers: Pyrenyl ester **7** is identical to **5** except that the glutamic acid residue is esterified by hydroxymethylpyrene rather than hydroxymethylbenzene. It was prepared specifically to be used as a probe of membrane insertion and dynamics. Pyrene fluorescence can afford information on the polarity of the environment experienced by the fluorophore and excimer formation, when it is observed, indicates association. The experimental studies are described below. First, however, it was essential to demonstrate that the presence of a pyrenyl ester did not alter the Cl[−] transport behavior of the SAT. Figure 8 shows

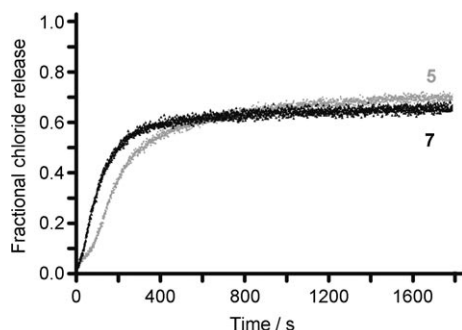


Figure 8. Fractional chloride release from DOPC/DOPA liposomes mediated by **5** and **7**.

the fractional chloride release from liposomes mediated by benzyl ester **5** and by pyrenylmethyl ester **7**. The curves are not identical, but they are nearly so. If anything, the pyrenylmethyl ester appears to give a cleaner sigmoidal release than **5**.

The fluorescence spectrum of **7** was determined in aqueous HEPES buffer in the concentration range 0.25 to 3.72 μM by using an excitation wavelength of 345 nm (Figure 9). The major band was centered at ≈ 470 nm in all spectra. This broad band is typical of excimer formation for pyrene, which suggests aggregation of the amphiphiles in

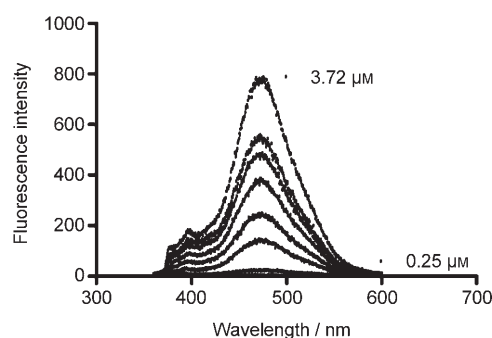


Figure 9. Fluorescence titration curves determined in HEPES buffer for **7**. The concentrations of **7** used were, from bottom to top, 0.25, 0.62, 1.25, 1.87, 2.49, 3.10, and 3.72 μM . The excitation wavelength was 345 nm.

aqueous solution. A plot of fluorescence intensity versus concentration was linear ($R^2 = 0.99$, data not shown).

Formation of the well-known pyrene excimer by amphiphilic **7** in a polar solvent was not surprising. However, we wished to determine if aggregation was controlled by the ionophoric peptide rather than by pyrene at these concentrations. Fluorescence spectra were therefore determined for 1-pyrenylmethanol (Figure 10a) and for **7** (Figure 10b) in CH_2Cl_2 , EtOH, and HEPES buffer. The concentrations of 1-pyrenylmethanol (0.62 μM) and **7** (1.25 μM) were adjusted to afford similar fluorescent intensities and thereby to facilitate comparison. In these solvents at these concentrations, only **7** showed an excimer band. No excimer band was detected for

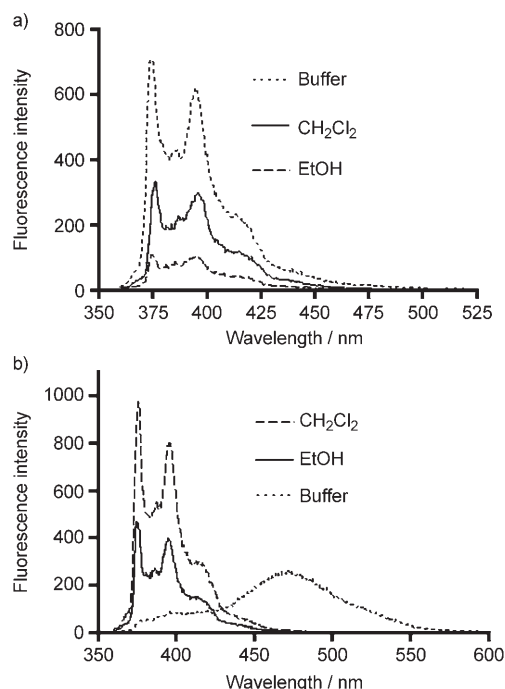


Figure 10. a) Solvent dependence of 1-pyrenylmethanol in HEPES buffer, CH_2Cl_2 , and EtOH. b) Solvent dependence of **7** in HEPES buffer, CH_2Cl_2 , and EtOH. The excimer band centered at $\lambda = 470$ nm is observed only for **7** in aqueous buffer.

1-pyrenylmethanol in buffer, CH_2Cl_2 , or ethanol. The intensities of the spectra diminished in the order HEPES > CH_2Cl_2 > EtOH. The approximate dielectric constants of these solvents are 80 in aqueous buffer, 24 in EtOH, and 5 in CH_2Cl_2 . Thus, the spectral intensity order does not follow the polarity order, which suggests that other forces are at work.

The striking difference in solvent dependence between 1-pyrenylmethanol and **7** shows that aggregation results from peptide interactions rather than an aggregation of pyrene itself. Of course, the excimer emission shows that pyrene-pyrene contact occurs in **7**, even though many other residues are present. The aggregation suggests that **7** dimerizes or oligomerizes in aqueous suspension before inserting into a vesicular membrane.

Two comparisons are of interest concerning Figure 11. First, we note that there is relatively little difference in the fluorescence spectra obtained for **7** in DOPC vesicles (Fig-

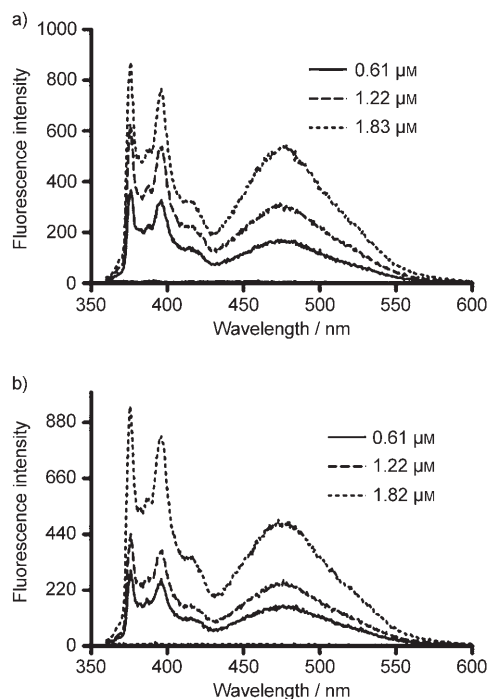


Figure 11. a) Fluorescence spectra of **7** in DOPC liposomes (0.31 mM) suspended in HEPES buffer. b) Fluorescence spectra of **7** in DOPC-DOPA liposomes (0.31 mM) suspended in HEPES buffer.

ure 11a) compared to liposomes formed from 7:3 DOPC/DOPA (Figure 11b). DOPA has an anionic head group and DOPC has a cationic head group. Differences in amphiphile insertion into the membrane and/or aggregation of the ionophores might have been apparent, but were not. Similar results were obtained for Cl^- release from the two different types of liposomes (data not shown).

Divergence in behavior is more apparent when the fluorescence spectra of **7**, obtained in solutions or vesicular suspension, are compared. Compound **7** showed excimer for-

mation in homogeneous solution only in aqueous buffer and not in CH_2Cl_2 or EtOH (Figure 10b). When the excimer of **7** was observed in HEPES buffer, no monomer peak was apparent. In either liposomal preparation, however, monomer and excimer peaks were observed. Our interpretation of these observations is that **7** aggregates to form at least dimers in aqueous solution. These dimers or oligomers then contact the liposome surface and partition into the membrane where they form pores. The overall process must be rapid because both Cl^- and CF^- release are detected rapidly. To the extent that monomer and dimer both exist in the bilayer, the equilibrium could account for the observed open-close behavior (see below) of the synthetic channels.

To further determine if excimer formation influenced aggregation and/or pore formation, a solution of **7** (1.87 μM) was titrated with $(\text{C}_{18}\text{H}_{37})_2\text{NCOCH}_2\text{OCH}_2\text{CO}-(\text{Gly})_3\text{-Pro}-(\text{Gly})_3\text{-O}(\text{CH}_2)\text{CH}_3$ (**8**). The latter is nonfluorescent, but structurally similar to **7**. The amounts of **8** added ranged from about two to twenty equivalents. As the amount of **8** increased, the fluorescence arising from the monomer increased. The monomer/excimer intensity ratio was measured. The fluorescence intensity ratio was plotted as a function of concentration (0–40 μM). A straight line (slope 0.05) was obtained with an R^2 value of 0.97. We thus infer that **7** behaves in a similar manner to other amphiphilic ionophores in this class and pyrene serves effectively as a reporter.

Planar bilayer conductance: The formation of ion-conducting pores and channels can be distinguished from the action of carrier molecules by using planar bilayer conductance methods. In this experiment, a bilayer membrane is created in a plate that separates two aqueous salt reservoirs. The bilayer membrane is an insulator in the absence of added ionophore. Thereafter, ion transport may be observed and monitored. Figure 12 shows a representative group of recordings obtained when **6** was added to a DOPC/DOPA (2:1 mol/mol, 7:3 w/w) membrane. The two reservoirs (cuvette and chamber) each contained a KCl (450 mM) buffer solution (10 mM HEPES, pH 7).

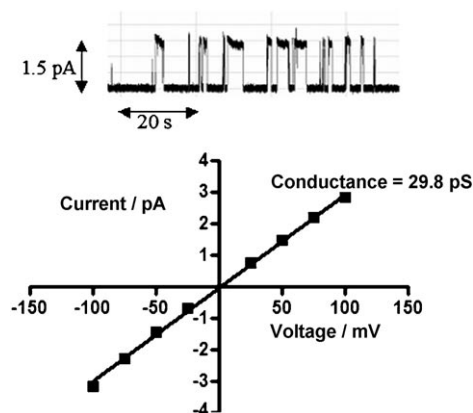


Figure 12. Planar bilayer conductance results for **6** in DOPC/DOPA bilayer membranes.

The recordings shown clearly illustrate that the channels or pores formed have regular, open–close states. The recordings shown here illustrate the predominant conductance state. During analyses of this system, more than one conductance state was observed, which is not surprising because multiple monomers may interact to give different pores simultaneously. The Hill analysis suggests that at least two monomers are involved in the formation of a pore. Thus, both 2- and 3-monomer pores are reasonable and expected. Of course, the ion release plots shown in this paper illustrate the average release over time from all pores that occur within the liposomes. A plot of current versus voltage (I – V curve) gave the expected straight line, which indicated that the pore was nonrectifying. The conductance calculated for the state illustrated in Figure 12 is 29.8 pS. Two other states were observed in different experiments that had conductance values of ≈ 6 and ≈ 100 pS.

Conclusion

The family of amphiphilic heptapeptides presented herein insert into phospholipid bilayers and form anion-conducting pores. These pores are at least dimeric, and planar bilayer experiments show that more than one conductance state may form. Ion-selective electrode and fluorescence techniques showed that chloride and carboxyfluorescein anions pass through the pores and the behavior of the average pore varies with the position of glutamate. Activity is highest when the glutamate residue is farthest from the central proline bend (i.e., closest to the C terminus). This suggests that charge is most influential when it is closest to the center of the ion pathway. Activity is also higher for glutamate esters than for the free carboxylate residue irrespective of the glutamate position. The influence of carboxyl compared with ester is largest for ^5Glx and ^7Glx , the two residues known from previous NMR studies to involve direct NH contact to anions.

As noted above, **7** is identical to **5** except that the glutamate residue is esterified by 1-pyrenemethanol rather than benzyl alcohol. Despite the significantly larger size of the aromatic residue, Cl^- transport by these two compounds is similar. This is an important observation because concern is sometimes expressed that the presence of a fluorescent residue necessarily alters the experiment. In the present case, esterification by hydroxymethylpyrene rather than hydroxymethylbenzene shows no deleterious effect. On the contrary, the fluorescence of pyrene permits an assessment of the environment it experiences within the liposome or in aqueous suspension. The assembly of peptide amphiphiles and insertion into liposomes can be monitored by the intensity changes observed in the monomer and excimer peaks.

Although these compounds are dynamic pore formers, the influence of the glutamate residue on ion transport is clearly in evidence. The presence of the negatively charged side chain within the heptapeptide sequence clearly diminished Cl^- transport. An attempt was made to reverse the negative

charge effect in these heptapeptides by preparing liposomes at pH 4. At this pH, glutamate should be largely protonated and differences between acid and ester should be minimized. Unfortunately, at pH 4, the vesicles proved to be unstable.

Negative ion ES-MS has clearly shown that chloride ion binding occurs with the neutral ionophoric peptides, but less well when a free carboxyl is present. Selectivity studies showed that the self-assembled pores favor Cl^- over K^+ transport even when the free and ionizable carboxyl group is present on the peptide. It is proposed that the Cl^- proteins have a similar electrostatic influence in their ion-conduction pathway. It is postulated that in the closed state the pore is blocked by E-148 by a hydrogen-bond interaction with the main-chain amide. The possibility that glutamate could serve as a charged gate in a more rigid protein system is certainly plausible in light of the present results.

Experimental Section

General: ^1H NMR spectra were recorded in CDCl_3 unless otherwise specified at 300 MHz on a Varian Gemini 300 MHz NMR spectrometer and are reported in the following manner: chemical shifts reported in ppm (δ) downfield from internal $(\text{CH}_3)_4\text{Si}$ (multiplicity (br=broad, s=singlet, d=doublet, t=triplet, q=quartet, brs=broad singlet, m=multiplet, etc.), coupling constants in Hz, integrated intensity, assignment). ^{13}C NMR spectra (in CDCl_3 unless otherwise noted) were obtained at 75 MHz and are referenced to CDCl_3 (77.23 ppm). Infrared spectra were recorded by using a Perkin–Elmer 1710 Fourier transform infrared spectrometer. Melting points were determined on a Thomas Hoover apparatus in open capillaries and are uncorrected. Thin layer chromatography analyses were performed on silica gel 60-F-254 with a thickness of 0.2 mm. Preparative chromatography columns were packed with silica gel (Kieselgel 60, 70–230 mesh or Merck grade 9385, 230–400 mesh, 60 Å). Reagents were the best (non-LC) grade commercially available and were distilled, recrystallized, or used without further purification as appropriate. CH_2Cl_2 was distilled from calcium hydride. DGA represents diglycolyl, $\sim\text{COCH}_2\text{OCH}_2\text{CO}\sim$. Combustion analyses were performed by M-H-W Laboratories, Phoenix, AZ, and are reported as percentages.

Synthesis 18₂DGA-GGG-OH: Compound 18₂DGA-GGG-OH was prepared as previously reported.^[11d]

TsOH-GG-OC₇H₁₅: Glycylglycine (GG) (1.00 g, 7.57 mmol) and TsOH monohydrate (1.59 g, 8.36 mmol) were added to a mixture of 1-heptanol (4.5 mL, 31.8 mmol) and toluene (50 mL). The mixture was heated to reflux and water was removed by using a Dean–Stark adapter for 7 h. The mixture was cooled to room temperature, diluted with diethyl ether (50 mL) and cooled at 0°C overnight. The solid was collected and recrystallized from MeOH/Et₂O to give a white solid (2.46 g, 81%). M.p. 131–133°C; ^1H NMR (300 MHz, CDCl_3): δ =0.88 (t, $^3J(\text{H,H})$ =6.8 Hz, 3H; CH_2CH_3), 1.26 (*pseudo-s*, 8H; $\text{OCH}_2\text{CH}_2(\text{CH}_2)_4\text{CH}_3$), 1.52 (t, $^3J(\text{H,H})$ =6.6 Hz, 2H; $\text{OCH}_2\text{CH}_2(\text{CH}_2)_4\text{CH}_3$), 2.29 (s, 3H; $\text{CH}_3\text{C}_6\text{H}_4\text{SO}_3$), 3.77 (d, $^3J(\text{H,H})$ =5.1 Hz, 2H; Gly CH_2), 3.95–4.00 (m, 4H; Gly CH_2 and $\text{OCH}_2\text{CH}_2(\text{CH}_2)_4\text{CH}_3$), 7.01 (d, $^3J(\text{H,H})$ =8.1 Hz, 2H; Tosyl H_{Ar}), 7.64–7.53 (m, 5H; Tosyl H_{Ar} and Gly NH_3), 8.10 ppm (t, $^3J(\text{H,H})$ =5.4 Hz, 1H; Gly NH); ^{13}C NMR (75 MHz, CDCl_3): δ =14.3, 21.5, 22.8, 26.0, 28.6, 29.2, 31.9, 41.3, 65.8, 126.2, 129.2, 140.5, 141.3, 167.1, 170.0 ppm; IR (CHCl_3): 3299, 3164, 2956, 2931, 2858, 1758, 1697, 1575, 1513, 1467, 1442, 1397, 1375, 1323, 1279, 1216, 1170, 1124, 1037, 1011 cm^{-1} .

Boc-E(γ -benzyl ester)GG-OC₇H₁₅: TsOH-GG-OC₇H₁₅ (0.60 g, 1.49 mmol), Boc-E- γ -benzyl ester (0.50 g, 1.49 mmol), EDCI (0.31 g, 1.64 mmol), and HOBt (0.22 g, 1.64 mol) were dissolved in CH_2Cl_2 (40 mL) and Et₃N (0.62 mL) was added. The mixture was stirred at 0°C for 0.5 h, at RT for 12 h, and the solvent was evaporated in vacuo. The

a solution (1 mM) in 2-propanol with mixing to the desired concentration. Dequenching, F_{520} , was computed as the fraction of total release upon addition of 2% aqueous solution of Triton X100 (100 μ L) and is shown in Equation (1):

$$F_{520} = \frac{F - F_0}{F_{\text{Triton}} - F_0} \quad (1)$$

in which F_0 is the fluorescence at time zero and F_{Triton} is the fluorescence after Triton addition. The data was fitted to a sigmoidal equation (by using OriginPro 7), that is, $y = A[x^n/(k^n + x^n)]$. In this equation, k is the time constant, which is the inverse of the rate constant for the pore formation process.

Fluorescence spectroscopy: Fluorescence was measured by using a Perkin-Elmer LS50B fluorimeter to evaluate continuously stirred samples. A stock solution of **7** (0.50 mM) in 2-propanol was prepared. 1-Pyrenemethanol (0.50 mM in 2-propanol) was used as a control. Compound **7** was added and stirred for about 60 s before spectra were recorded. Except where indicated in the text or figure caption, the emission spectrum for **7** was measured in external buffer (2 mL, K_2SO_4 (400 mM), HEPES (10 mM), pH 7.0) and the exact concentration of **7** was shown in the figure. For solvent dependence experiments, freshly distilled solvent (2 mL) instead of buffer was used and the concentration of **7** was adjusted for the instrument capacity. For measurements in the vesicles, compound **7** was added to the liposome suspension (as prepared above, in external buffer (2 mL)) and the overall lipid concentration was 0.31 mM (same as chloride release experiment). An aliquot of stock solution of **7** was added to achieve the desired concentration. The excitation wavelength was $\lambda = 345$ nm and the emission spectrum was recorded between $\lambda = 300$ and 600 nm (2.5 nm slit width, 400 nm min⁻¹ scan speed, average three scans).

Planar bilayer measurements: Bilayer measurements were performed with a Warner BC-525D bilayer clamp apparatus. Planar membranes were formed by painting lipids (DOPC/DOPA 2:1 mol/mol, 20 mg mL⁻¹ in *n*-decane) over a 200 mm aperture on the side of a cuvette fitted into a chamber. The cuvette and chamber contained a KCl (450 mM) buffer solution (HEPES (10 mM), pH 7). After membrane formation was ascertained (membranes with a capacitance lower than 100 pF were discarded), an aliquot of a solution of the compound being studied (in TFE) was added to a suspension of vesicles (20 mM) in the same buffer (vesicles were previously prepared by using the same lipid composition and the same buffer used for the bilayer experiments). An aliquot of this solution was then stirred into the buffer on the chamber side ("cis" side to where the reference electrode is immersed ("ground")) to achieve the desired concentration. Records were filtered with a 4-pole Bessel filter (100 Hz) and digitized at a 1 kHz sampling interval per signal by using Clampex 9.2 (Axon instruments). Data analysis was performed with Clampfit 9.2 (Axon Instruments).

Computational details: Calculations were performed by using the Gaussian 03^[19] suite of programs. Semi-empirical (PM3) and density functional (B3LYP) methods were used to optimize the geometries and perform frequency analysis. The B3LYP method combines Becke's three-parameter function^[26] with the nonlocal correlation provided by the correlation function of Lee, Yang, and Parr,^[27] which is suitable for vibrational calculations.

Negative ion mass spectrometry: Mass spectra were obtained by using a JEOL MStation (JMS-700) mass spectrometer equipped with an electrospray ionization source, which operated in the negative ion mode and scanning from m/z 600 to 2400. Slits were set to achieve a resolution of about 2000. The spray voltage was 2.00 kV, and the capillary temperature (desolvating temperature) was 200 °C. Each trial was processed by using the MSMP9020D software supplied by JEOL with a minimum of ten scans averaged for the final spectral presentation.

Acknowledgement

We thank the NIH for grants (GM 36262, GM 63190) to support this work.

- [1] A. Bianchi, K. Bowman-James, E. Garcia-España, *Supramolecular chemistry of anions*, Wiley-VCH: New York, **1997** p. 461.
- [2] F. P. Schmidtchen, M. Berger, *Chem. Rev.* **1997**, *97*, 1609–1648.
- [3] P. D. Beer, P. A. Gale, *Angew. Chem.* **2001**, *113*, 502–532; *Angew. Chem. Int. Ed.* **2001**, *40*, 486–516.
- [4] *Anion coordination chemistry II, Vol. 250* (Ed.: P. A. Gale), Elsevier, Amsterdam, **2006**; .
- [5] a) K. Bowman-James, *Acc. Chem. Res.* **2005**, *38*, 671–678; b) S. O. Kang, R. A. Begum, K. Bowman-James, *Angew. Chem.* **2006**, *118*, 8048–8061; *Angew. Chem. Int. Ed.* **2006**, *45*, 7882–7894.
- [6] J. L. Sessler, D. E. Gross, W. S. Cho, V. M. Lynch, F. P. Schmidtchen, G. W. Bates, M. E. Light, P. A. Gale, *J. Am. Chem. Soc.* **2006**, *128*, 12281–12288.
- [7] a) P. A. Gale, *Acc. Chem. Res.* **2006**, *39*, 465–475; b) J. L. Sessler, P. A. Gale, W.-S. Cho, *Anion Receptor Chemistry*, RSC, Cambridge, **2006**.
- [8] A. P. Davis, D. N. Sheppard, B. D. Smith, *Chem. Soc. Rev.* **2007**, *36*, 348–357.
- [9] a) A. Accardi, C. Miller, *Nature* **2004**, *427*, 803–807; b) A. Accardi, M. Walden, W. Nguitragool, H. Jayaram, C. Williams, C. Miller, *J. Gen. Physiol.* **2005**, *126*, 563–570.
- [10] C. Miller, *Science* **2006**, *312*, 534–535.
- [11] C. Miller, *Nature* **2006**, *440*, 484–489.
- [12] O. Scheel, A. A. Zdebik, S. Lourdel, T. J. Jentsch, *Nature* **2005**, *436*, 424–427.
- [13] R. Dutzler, E. B. Campbell, M. Cadene, B. T. Chait, R. MacKinnon, *Nature* **2002**, *415*, 287–294.
- [14] a) R. Dutzler, E. B. Campbell, R. MacKinnon, *Science* **2003**, *300*, 108–112; b) R. Dutzler, *FEBS Lett.* **2004**, *564*, 229–233.
- [15] a) P. H. Schlesinger, R. Ferdani, R. Pajewski, J. Pajewska, G. W. Gokel, *Chem. Commun.* **2002**, 840–841; b) P. H. Schlesinger, R. Ferdani, J. Liu, J. Pajewska, R. Pajewski, M. Saito, H. Shabany, G. W. Gokel, *J. Am. Chem. Soc.* **2002**, *124*, 1848–1849; c) N. Djedovic, R. Ferdani, E. Harder, J. Pajewska, R. Pajewski, P. H. Schlesinger, G. W. Gokel, *Chem. Commun.* **2003**, 2862–2863; d) P. H. Schlesinger, R. Ferdani, J. Pajewska, R. Pajewski, G. W. Gokel, *New J. Chem.* **2003**, *27*, 60–67; e) P. H. Schlesinger, N. K. Djedovic, R. Ferdani, J. Pajewska, R. Pajewski, G. W. Gokel, *Chem. Commun.* **2003**, 308–309; f) G. W. Gokel, P. H. Schlesinger, N. K. Djedovic, R. Ferdani, E. C. Harder, J. Hu, W. M. Leevy, J. Pajewska, R. Pajewski, M. E. Weber, *Bioorg. Med. Chem.* **2004**, *12*, 1291–1304; g) R. Pajewski, R. Ferdani, P. H. Schlesinger, G. W. Gokel, *Chem. Commun.* **2004**, 160–161; h) N. Djedovic, R. Ferdani, E. Harder, J. Pajewska, R. Pajewski, M. E. Weber, P. H. Schlesinger, G. W. Gokel, *New J. Chem.* **2005**, *29*, 291–305; i) R. Ferdani, R. Pajewski, N. Djedovic, J. Pajewska, P. H. Schlesinger, G. W. Gokel, *New J. Chem.* **2005**, *29*, 673–680; j) R. Pajewski, R. Ferdani, J. Pajewska, N. Djedovic, P. H. Schlesinger, G. W. Gokel, *Org. Biomol. Chem.* **2005**, *3*, 619–625; k) R. Pajewski, R. Ferdani, J. Pajewska, R. Li, G. W. Gokel, *J. Am. Chem. Soc.* **2005**, *127*, 18281–18295; l) G. A. Cook, R. Pajewski, M. Aburi, P. E. Smith, O. Prakash, J. M. Tomich, G. W. Gokel, *J. Am. Chem. Soc.* **2006**, *128*, 1633–1638; m) R. Pajewski, R. Garcia-Medina, S. L. Brody, P. H. Schlesinger, G. W. Gokel, *Chem. Commun.* **2006**, 329–331; n) L. You, R. Ferdani, G. W. Gokel, *Chem. Commun.* **2006**, 603–605.
- [16] P. Yeagle, *The Structure of Biological Membranes*, CRC, Boca Raton, **1992**, p. 1227.
- [17] a) L. Yang, T. A. Harroun, T. M. Weiss, L. Ding, H. W. Huang, *Bio-phys. J.* **2001**, *81*, 1475–1485; b) H. W. Huang, F.-Y. Chen, M.-T. Lee, *Phys. Rev. Lett.* **2004**, *92*, 198304.
- [18] R. Dutzler, *Curr. Opin. Struct. Biol.* **2006**, *16*, 439–446.
- [19] Gaussian 03, Revision A.1, M. J. Frisch, G. W. Trucks, H. B. Schlegel, G. E. Scuseria, M. A. Robb, J. R. Cheeseman, J. A. Mont-

- gomery, Jr., T. Vreven, K. N. Kudin, J. C. Burant, J. M. Millam, S. S. Iyengar, J. Tomasi, V. Barone, B. Mennucci, M. Cossi, G. Scalmani, N. Rega, G. A. Petersson, H. Nakatsuji, M. Hada, M. Ehara, K. Toyota, R. Fukuda, J. Hasegawa, M. Ishida, T. Nakajima, Y. Honda, O. Kitao, H. Nakai, M. Klene, X. Li, J. E. Knox, H. P. Hratchian, J. B. Cross, V. Bakken, C. Adamo, J. Jaramillo, R. Gomperts, R. E. Stratmann, O. Yazyev, A. J. Austin, R. Cammi, C. Pomelli, J. W. Ochterski, P. Y. Ayala, K. Morokuma, G. A. Voth, P. Salvador, J. J. Dannenberg, V. G. Zakrzewski, S. Dapprich, A. D. Daniels, M. C. Strain, O. Farkas, D. K. Malick, A. D. Rabuck, K. Raghavachari, J. B. Foresman, J. V. Ortiz, Q. Cui, A. G. Baboul, S. Clifford, J. Cio-slowski, B. B. Stefanov, G. Liu, A. Liashenko, P. Piskorz, I. Komaromi, R. L. Martin, D. J. Fox, T. Keith, M. A. Al-Laham, C. Y. Peng, A. Nanayakkara, M. Challacombe, P. M. W. Gill, B. Johnson, W. Chen, M. W. Wong, C. Gonzalez, J. A. Pople, Gaussian, Inc., Wallingford CT, **2004**.
- [20] P. Berndt, G. B. Fields, M. Tirrell, *J. Am. Chem. Soc.* **1995**, *117*, 9515–9522.
- [21] A. F. Chu-Kung, K. N. Bozzelli, N. A. Lockwood, J. R. Haseman, K. H. Mayo, M. V. Tirrell, *Bioconjugate Chem.* **2004**, *15*, 530–535.
- [22] S. Kubik, R. Kirchner, D. Nolting, J. Seidel, *J. Am. Chem. Soc.* **2002**, *124*, 12752–12760.
- [23] R. Ferdani, R. Li, R. Pajewski, J. Pajewska, R. E. K. Winter, G. W. Gokel, *Org. Biomol. Chem.* **2007**, *5*, 2423–2432.
- [24] A. G. Harrison, J. Malat, *Int. J. Mass Spectrom. Ion Proc.* **1997**, *167–168*, 213–221.
- [25] I. Segel, *Enzyme Kinetics: Behavior and Analysis of Rapid Equilibrium and Steady-State Enzyme Systems*. Wiley, New York, **1993**, pp. 371–375.
- [26] A. D. Becke, *J. Chem. Phys.* **1993**, *98*, 5648–5652.
- [27] C. Lee, W. Yang, R. G. Parr, *Phys. Rev. B* **1988**, *37*, 785–789.

Received: July 12, 2007
Published online: October 10, 2007